Evaluation of Bacterial RNase P RNA as a Drug Target

Dagmar K. Willkomm,[a] Heike Gruegelsiepe,[a] Olga Goudinakis,[b] Rosel Kretschmer-Kazemi Far,[c] Rolf Bald,[d] Volker A. Erdmann,[d] and Roland K. Hartmann*[a]

RNA has gained increasing importance as a therapeutic target. However, so far mRNAs rather than stable cellular RNAs have been considered in such studies. In bacteria, the tRNA-processing enzyme RNase P has a catalytic RNA subunit. Fundamental differences in structure and function between bacterial and eukaryotic RNase P, and its indispensability for cell viability make the bacterial enzyme an attractive drug target candidate. Herein we describe two approaches utilized to evaluate whether the catalytic RNA subunit of bacterial RNase P is amenable to inactivation by antisense-based strategies. In the first approach, we rationally designed RNA hairpin oligonucleotides targeted at the tRNA 3′-CCA binding site (P15 loop region) of bacterial RNase P RNA by attempting to include principles derived from the natural CopA – CopT antisense system. Substantial inactivation of RNase P RNA was observed for Type A RNase P RNA (such as that in Escherichia coli*) but not for Type B (as in* Mycoplasma hyopneumoniae*). Moreover, only an RNA oligonucleotide (Eco 3′) complementary to the CCA binding site and its 3′ flanking sequences was shown to be an efficient inhibitor. Mutation of Eco 3′ and analysis of other natural RNase P RNAs with sequence deviations in the P15 loop region showed that inhibition is due to interaction of Eco 3′ with this region and occurs in a highly sequence-specific manner. A DNA version of Eco 3′ was a less potent inhibitor. The potential of Eco 3′ to form an initial kissing complex with the P15 loop did not prove advantageous. In a second approach, we tested a set of oligonucleotides against* E. coli *RNase P RNA which were designed by algorithms developed for the selection of suitable mRNA targets. This approach identified the P10/11-J11/12 region of bacterial RNase P RNA as another accessible region. In conclusion, both the P15 loop and P10/11-J11/12 regions of Type A RNase P RNAs seem to be promising antisense target sites since they are easily accessible and sufficiently interspersed with nonhelical sequence elements, and oligonucleotide binding directly interferes with substrate docking to these two regions.*

Introduction

Endonucleolytic 5′ maturation of tRNA primary transcripts, one of the prerequisites of protein synthesis, is catalyzed by the ribonucleoprotein enzyme ribonuclease P (RNase P) in all three kingdoms of life (Archaea, Bacteria, and Eukarya), as well as in mitochondria and chloroplasts.[1–3] The enzyme has been shown to be essential for cell viability in pro- and eukaryotes.[1, 4, 5] Recently, systematic inactivation of *Bacillus subtilis* genes has revealed that the genes for RNase P components belong to the relatively small fraction of genes (about 300 out of 4100 tested) that are indispensable for bacterial life.[6] The RNase P enzymes of bacteria are composed of a catalytic RNA subunit about 400 nucleotides in length, and a single small protein that contributes only 10% to the mass of the holoenzyme.[7] An RNA subunit of similar size is found in archaea, eukaryotic nuclei, and many mitochondria.[7] However, in contrast to bacterial RNase P, archaeal and eukaryotic nuclear RNase P enzymes contain multiple protein subunits that make up more than 50% of the holoenzyme mass (for example, nine protein subunits in *Saccharomyces cerevisiae* and ten in *Homo sapiens*).[4, 5] The striking differences in bacterial and eukaryotic RNase P architecture entail functional consequences. First, bacterial RNase P RNA subunits can sustain catalytic activity in vitro in the absence of the protein complement, but their eukaryotic counterparts cannot.[1–3] Second, substrate recognition by bacterial RNase P enzymes involves multiple RNA – RNA interactions, whereas protein – RNA contacts seem to prevail in eukaryotic systems. For example, cross-linking studies utilizing 4-thio-uridine-labeled precursor tRNA (ptRNA) have revealed photoadducts of ptRNA with protein subunits of eukaryotic RNase P enzymes, but not

[a] *Prof. Dr. R. K. Hartmann, Dr. D. K. Willkomm, H. Gruegelsiepe*
Philipps-Universität Marburg
Institut für Pharmazeutische Chemie
Marbacher Weg 6, 35037 Marburg (Germany)
Fax: (+49) 6421-282-5854
E-mail: hartmanr@staff.uni-marburg.de

[b] *O. Goudinakis*
Universität zu Lübeck
Institut für Biochemie
Ratzeburger Allee 160, 23538 Lübeck (Germany)

[c] *Dr. R. Kretschmer-Kazemi Far*
Universität zu Lübeck
Institut für Molekulare Medizin
Ratzeburger Allee 160, 23538 Lübeck (Germany)

[d] *PD Dr. R. Bald, Prof. Dr. V. A. Erdmann*
Freie Universität Berlin
Institut für Biochemie
Thielallee 63, 14195 Berlin (Germany)

 DOI: 10.1002/cbic.200300674

with their RNA subunits.[8] In contrast, photoadducts were only detected with the RNA component in parallel control experiments with the RNase P holoenzyme from *Escherichia coli*.[8] One RNA–RNA contact between ptRNA substrates and many bacterial RNase P RNAs involves the 3′-CCA terminus of the tRNA body and a specific internal loop of RNase P RNA, referred to as the P15 loop. Two conserved G residues within this loop form Watson–Crick base pairs with the two consecutive C residues of the CCA motif.[2, 9–11] Eukaryotic RNase P enzymes apparently lack a corresponding binding site for tRNA 3′-CCA termini, neither do their RNA subunits have the structural equivalent of the bacterial P15 loop that would be able to base-pair with the substrate 3′-CCA motif. This observation explains why this element is unimportant in determining enzyme efficiency in eukaryotic systems.[2] It is also consistent with the fact that eukaryotic ptRNA primary transcripts carry a polyuridine stretch as their 3′-trailing sequence and initially lack a 3′-CCA sequence.[5]

RNA is becoming an increasingly important therapeutic target. However, mainstream approaches have so far focused on mRNAs, whereas structured RNAs have been largely neglected as targets in antisense-based investigations. In strategies against bacteria, for which catalytic RNAi machineries are not available, antisense-related approaches represent a serious but little-explored option. Bacterial RNase P combines several favorable target features. It contains a stable catalytic RNA subunit with limited turnover relative to many mRNAs, which leads to the prediction that inactivation of this subunit will result in a rather persistent phenotype. Also, the enzyme is a highly efficient catalyst, consistent with its generally low cellular abundance.[1] For example, *E. coli* cells contain a 60 to 100-fold molar excess of ribosomes over RNase P RNA.[12] Thus, lower intracellular drug concentrations should be required for inactivation of RNase P relative to the concentrations required for ribosomes. In comparison with tRNAs, another class of potential RNA targets essential for protein synthesis, RNase P RNA has the advantage of having a larger sequence space than tRNA. This fact, the high sequence similarities between different tRNA species, and the particularly rigid architecture of tRNA molecules predict that specificity and efficacy of antisense interaction will be superior for RNase P RNA compared with tRNA. Finally, the difference in structure and function between bacterial and eukaryotic RNase P enzymes provides a further argument in favor of strategies that aim at combatting bacterial pathogens by inactivating their essential RNase P activity while leaving the human enzyme unaffected. With a similar goal in mind, Gopalan and coworkers[13] recently tested the inhibition of bacterial RNase P by aminoglycoside–arginine conjugates. Such arginine derivatives were found to be more potent inhibitors than the corresponding aminoglycosides themselves and, moreover, inhibited human RNase P to a substantially lower extent than RNase P from *E. coli*.[13]

Herein, we describe two approaches that were pursued to evaluate whether bacterial RNase P can be inactivated by antisense-based strategies. In the first approach, we conceived a rational design directed against the CCA binding site. This region combines several features of a favorable target: it is part of the active site and thus crucial for enzyme function, is positioned at the enzyme periphery[14] and inferred to be easily accessible, and a comparable CCA binding site is missing in human RNase P. Furthermore, sequence variation around the CCA binding site among bacteria should allow steering of the specificity of antisense oligonucleotides with respect to the target organism.

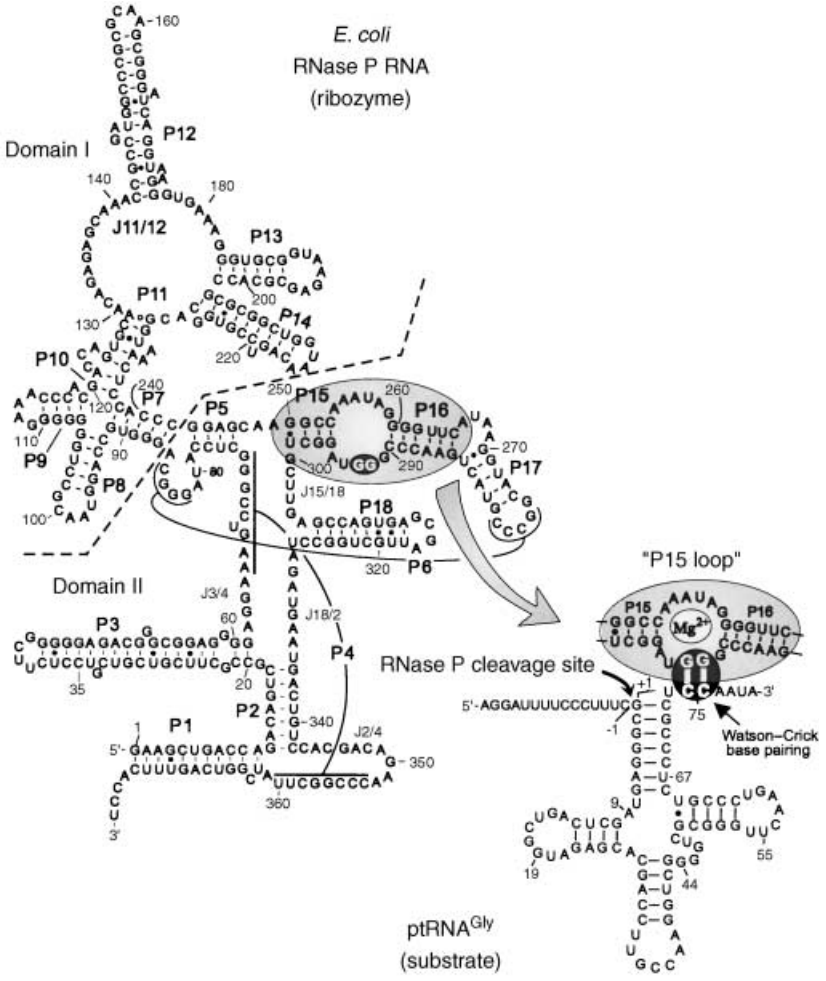

Figure 1. *Left: Secondary structure of* E. coli *RNase P RNA.[33] P, helical regions; J, joining segments named according to the numbers of the helices they connect. The grey-shaded oval depicts the P15/16 region including G292 and G293 (highlighted), which base pair to the CCA motif of a tRNA 3′ terminus.[9] The broken line separates the two main structural domains (Domain I or specificity domain; Domain II or catalytic domain[40]). Lower right: Interaction of a bacterial ptRNA^{Gly}[41] with the RNase P RNA "P15 loop". Highlighted nucleotides are involved in the two intermolecular Watson–Crick base pairs. The curved black arrow indicates the canonical RNase P cleavage site (between nucleotides -1 and $+1$). Two Mg^{2+} ions important for the cleavage process have been proposed to be bound in the P15 loop.[42]*

In the second approach, we tested a set of anti-*E. coli* RNase P RNA oligonucleotides selected by algorithms developed for mRNA targets.[15] In summary, our results indicate that the CCA binding region in the catalytic domain of Type A RNase P RNAs (such as in *E. coli*) is highly suitable for efficient target inactivation. Another promising target region for enzyme inactivation is located in the second so-called specificity domain of bacterial RNase P RNA.

Results and Discussion

Targeting of the CCA binding site

E. coli RNase P RNA has been the major model system for the study of RNase P RNA of the structural type A.[16] The secondary structure of this RNase P RNA as well as the interaction of the P15/16 subdomain with the 3′-CCA terminus of a ptRNA substrate is illustrated in Figure 1. In addition to *E. coli* RNase P RNA, we included the RNase P RNA from the swine lung pathogen *Mycoplasma hyopneumoniae*[17] in our analysis. The RNase P RNA of this organism is a representative of the second type (Type B) of RNase P RNA structures found among bacteria. A mutational analysis has provided evidence that this RNA also base pairs with the 3′-terminal CCA motif of tRNAs in ribozyme–substrate complexes.[18]

Our initial strategy for antisense oligonucleotide design was adapted from a well-characterized natural RNA–antisense RNA interaction system, CopA–CopT, known to regulate *E. coli* R1 plasmid replication.[19, 20] The main features of this system are: 1) formation of an initial contact between the apical loops (kissing complex) of hairpin structures in the sense and antisense RNAs, followed by 2) mutual strand invasion of fully comple-

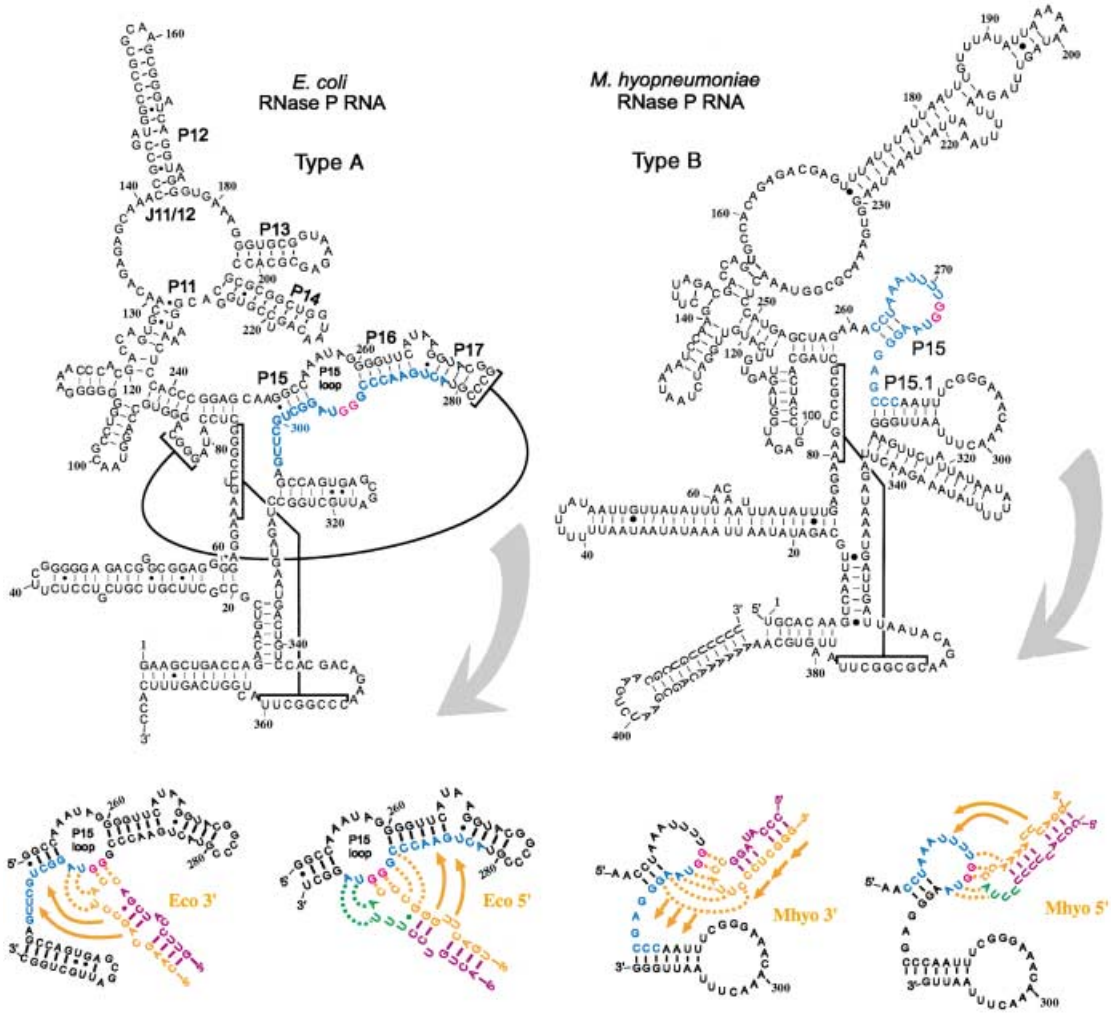

Figure 2. *Antisense inhibition strategies. Secondary structures of RNase P RNAs from* E. coli *(Type A) and* M. hyopneumoniae *(Type B) were taken from the RNase P database.[7] The designed RNA oligonucleotides (Eco 3′, Eco 5′, Mhyo 3′, and Mhyo 5′) and their direction of anticipated strand invasion are depicted at the bottom of the figure. The complementary sequences of the designed RNA oligonucleotides and the RNase P RNA are shown in dark yellow and blue, respectively. Note that only one side of the putative stem region of the hairpin oligonucleotides is complementary to nucleotides in RNase P RNA to avoid topological stress during strand invasion;[20] noncomplementary nucleotides are marked in purple. A so-called U-turn motif (YUNR; Y, pyrimidine; R, purine; N, any nucleotide), as found in CopT,[20] was introduced into the putative loop regions where possible (green nucleotides). This motif has been proposed to preform an A-helical conformation of loop nucleotides downstream of the conserved U residue and may thus improve binding specificity and rate.[20] The two conserved guanosine residues (G292/G293 in* E. coli *and G272/G273 in* M. hyopneumoniae *RNase P RNA) are shown in magenta.*

mentary sequences at the cost of concomitant disruption of hairpin stems 3) interspersed with bulged residues to lower their stability. It appears that the loop–loop kissing contact accelerates the association of sense and antisense RNAs, although rapid conversion to more stable complexes is essential to obtain maximum inhibition rates.[20]

By using this natural model system as the paradigm, we designed two RNA hairpin oligonucleotides directed against *E. coli* RNase P RNA, and two specific for *M. hyopneumoniae* RNase P RNA (Eco 5′, Eco 3′ and Mhyo 5′, Mhyo 3′, respectively; see Figure 2). These RNA oligonucleotides have the potential to form a kissing complex either with the P15 loop confined by helices P15 and P16 of *E. coli* RNase P RNA or with the structural equivalent of the *M. hyopneumoniae* ribozyme (Figure 2). Bulged residues in the hairpin stems were supposed to facilitate breaking of the intramolecular base pairs, which is a prerequisite for extended antisense–target interaction. Eco 5′ and Eco 3′ contain 14 and 13 nucleotides, respectively, that are complementary to G292/G293 of *E. coli* RNase P RNA and the 5′ or 3′ flanking sequences. Essentially the same is true for oligonucleotides Mhyo 5′ and Mhyo 3′ directed against G272/G273 in the P15 loop of *M. hyopneumoniae* RNase P RNA (Figure 2).

The four RNA oligonucleotides were tested as inhibitors in the ptRNA processing reactions catalyzed by *E. coli* and *M. hyopneumoniae* RNase P RNA (Figure 3 A and B). At a 100-fold molar excess (1 μM) relative to RNase P RNA, neither did Eco 5′ show significant inhibition of ptRNA cleavage by the *E. coli* ribozyme, nor did Mhyo 5′ or Mhyo 3′ cause any substantial inhibition of *M. hyopneumoniae* RNase P RNA. In contrast, essentially complete suppression of processing was observed at 1 μM Eco 3′ in the reaction catalyzed by *E. coli* RNase P RNA (Figure 3 A). The concentration of Eco 3′ required to obtain 50% inhibition (K_i value) was determined as 60 ± 30 nM (Figure 3 C). In control reactions under the same conditions, neither did Eco 3′ or Eco 5′ inhibit the *M. hyopneumoniae* ribozyme, nor did Mhyo 5′ or Mhyo 3′ show any effect on the *E. coli* ribozyme (data not shown).

The inefficiency of Eco 5′ may be explained by the necessity to disrupt the rather stable P16/17 helices of *E. coli* RNase P RNA for oligonucleotide invasion, which may have posed an insurmountable energetic barrier. It is less clear at present why we failed to see any effect of Mhyo 5′ or Mhyo 3′ on the reaction catalyzed by *M. hyopneumoniae* RNase P RNA. Here, disruption of the 3-bp P15 helix should be no more of a barrier for oligonucleotide invasion than in the case of Eco 3′, whose hybridization to *E. coli* RNase P RNA was expected to require disruption of the entire P15 helix. Mhyo 5′ and Mhyo 3′ inefficacy may be related to the low conformational rigidity (low G/C-content) of *M. hyopneumoniae* RNase P RNA or unfavorable constraints for oligonucleotide–P15 loop interaction.[21] In the case of Mhyo 3′, partial disruption of helix P15.1 may have posed an additional barrier (Figure 2).

Based on the aforementioned findings, further efforts were concentrated on the study of Eco 3′. We next tested a DNA version of Eco 3′, which was a much less efficient inhibitor (Figure 4) than the RNA oligonucleotide. As expected from the inefficiency of Eco 5′ RNA (Figure 3 A), a DNA version of Eco 5′ showed no effect on the processing reaction at a 100-fold excess (1 μM) relative to *E. coli* RNase P RNA (Figure 4).

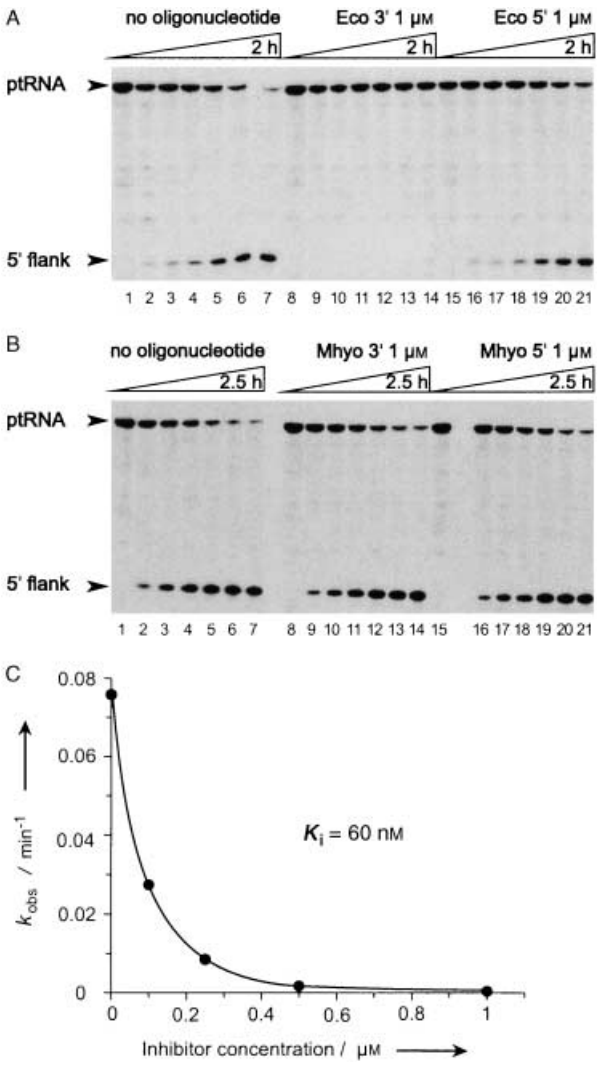

Figure 3. *A)* E. coli *RNase P RNA (10 nM) was preincubated in the presence or absence of the hairpin oligonucleotide Eco 3′ or Eco 5′ in cleavage assay buffer I at 37 °C for 40 min. A 100-fold molar excess of oligonucleotide (1.0 μM) over RNase P RNA was used. Processing reactions were started by addition of 5′-radiolabeled ptRNA^{Gly} substrate (100 nM). Aliquots were withdrawn at various time points (2, 5, 10, 30, 60, 120 min) and analyzed on 20% polyacrylamide/8 M urea gels; Lanes 1, 8, and 15 represent controls without RNase P RNA incubated for 120 min under the same conditions. Cleavage rates were inferred from the change in the ratio of released 5′ flank to ptRNA over time. B) Processing of ptRNA^{Gly} by* M. hyopneumoniae *RNase P RNA in the absence or presence of hairpin oligonucleotide Mhyo 3′ or Mhyo 5′. Experimental conditions were as in A, except that aliquots were withdrawn after 2, 5, 10, 30, 80, and 150 min. Lanes 1, 8, and 15 represent controls without RNase P RNA incubated for 150 min under the same conditions. C) Inhibition of ptRNA^{Gly} processing by* E. coli *RNase P RNA at different concentrations of RNA oligonucleotide Eco 3′ (data from one representative experiment). For assay conditions, see above and the Methods section.*

To ascertain whether inhibition of *E. coli* RNase P RNA was indeed due to interaction of Eco 3′ with the P15 region, we replaced the two C residues thought to pair with G292/G293 of *E. coli* RNase P with AA or UU dinucleotides. Both variants, Eco 3′ AA and Eco 3′ UU were substantially less effective inhibitors, which is consistent with our assumption that Eco 3′ interacts

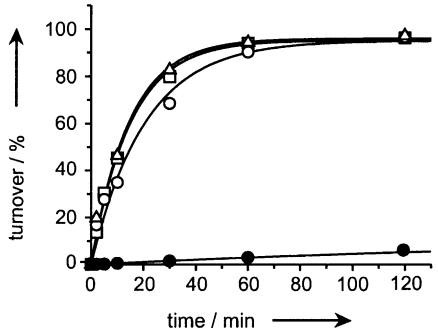

Figure 4. *Effects of DNA variants of Eco 3′ and Eco 5′ on ptRNA^{Gly} processing by* E. coli *RNase P RNA. Open squares, no inhibitor oligonucleotide; triangles, Eco 5′ DNA; open circles, Eco 3′ DNA; filled circles, Eco 3′ RNA. For assay conditions, see the legend of Figure 3 and the Methods section.*

with the P15 region (Figure 5). The higher inhibition efficiency of Eco 3′ UU relative to Eco 3′ AA can be explained by the capacity of the two U residues in Eco 3′ UU to form G·U wobble pairs with G292/G293. The aforementioned results of the mutational analysis predicted that natural RNase P RNAs with nucleotide exchanges in the target region should be much less or not at all affected by Eco 3′. This hypothesis was tested with the RNase P

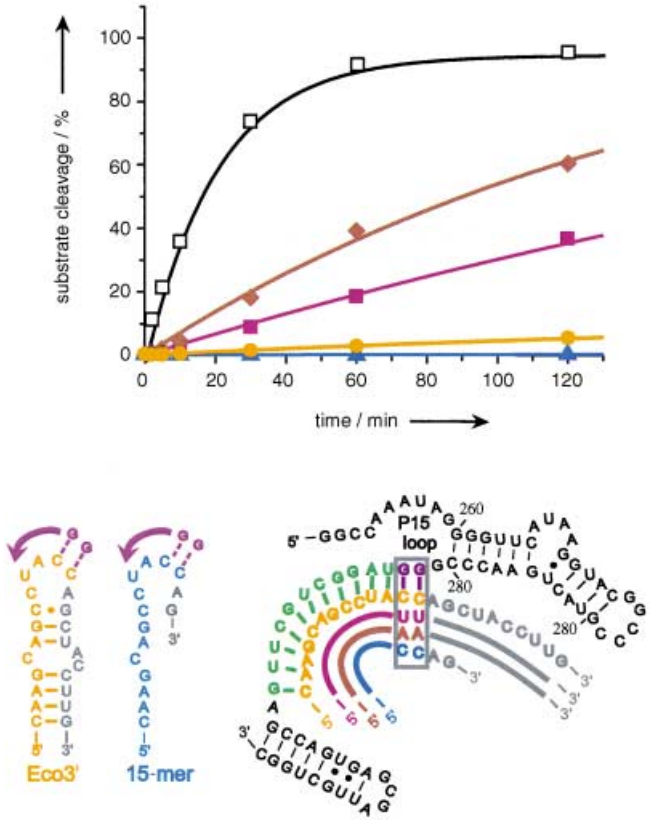

Figure 5. *Processing of ptRNA^{Gly} by* E. coli *RNase P RNA either in the absence of inhibitor (open squares) or in the presence of 1 μM Eco 3′ (dark yellow circles), Eco 3′ AA (brown diamonds), Eco 3′ UU (purple squares), or a shortened 15-mer variant (blue triangles). The RNA oligonucleotides are shown in complex with the P15 loop region at the bottom on the right. The putative structures of Eco 3′ and the 15-mer are illustrated on the left. For assay conditions, see the legend of Figure 3 and the Methods section.*

RNAs from *Thermus thermophilus* (Type A, as in *E. coli*) and *B. subtilis* (Type B, as in *M. hyopneumoniae*) under our standard assay conditions. Whereas processing by *E. coli* RNase P RNA was almost completely abolished by Eco 3′ (Figure 5), the two other RNase P RNAs remained entirely unaffected (Figure 6). Relative to *E. coli* RNase P RNA, the potential base-pairing capacity is

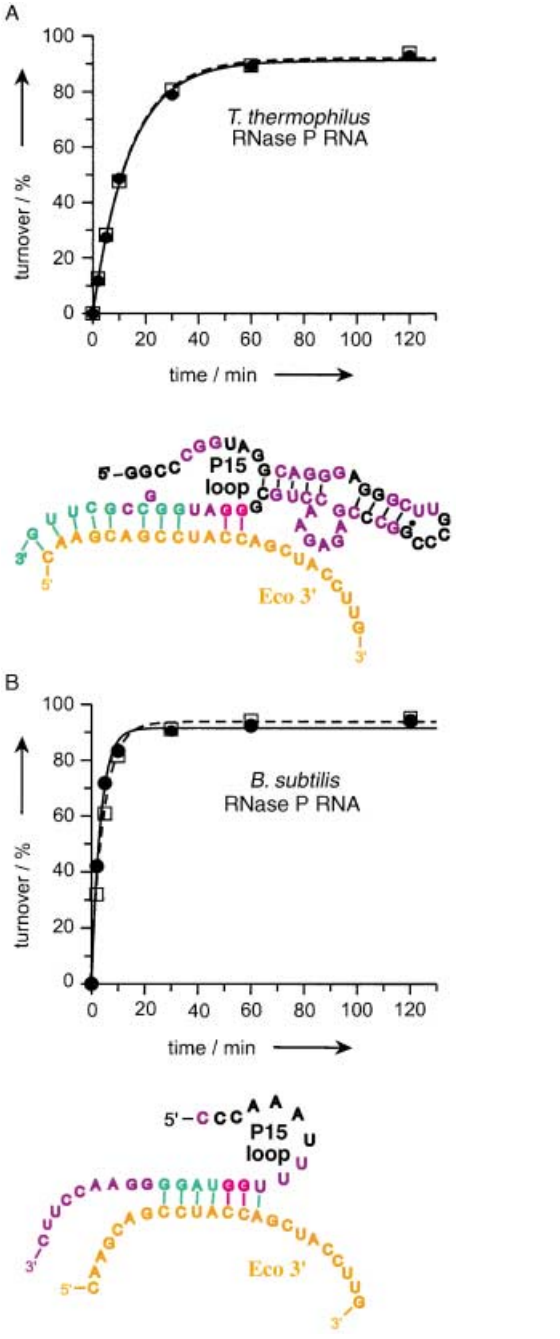

Figure 6. *Processing of ptRNA^{Gly} by* T. thermophilus *or* B. subtilis *RNase P RNA[7] either in the absence or presence of 1 μM Eco 3′. Assays were conducted as described in the legend of Figure 3. RNase P RNAs and Eco 3′ were preincubated for 20 min at 37 °C in buffer I. Nucleotides whose identities differ from those in* E. coli *RNase P RNA are shown in purple; the conserved G residues (G292/G293 in* E. coli *RNase P RNA) are highlighted in magenta; magenta and green nucleotides in* T. thermophilus *and* B. subtilis *RNase P RNAs are complementary to Eco 3′. For further details, see the Methods section.*

reduced from 13 to 6 consecutive bp in the case of the *B. subtilis* ribozyme, and hybrid formation with *T. thermophilus* RNase P RNA would be compromised by 3 mismatches and 1 bulged nucleotide (Figure 6A and B, lower parts). Thus, our results indicate that Eco 3′ indeed interacts with the P15 loop region and that formation of sense–antisense complexes is very sensitive to mismatches. Our results leave open the question of whether inhibition was due to intermolecular helix formation over the entire region of complementarity.

We also analyzed whether the potential of Eco 3′ to form a hairpin structure is crucial to inhibition efficacy. A 15-mer lacking the 3′-proximal part of the stem but retaining the complementary antisense sequence portion turned out to be even more effective than Eco 3′ (Figure 5). This result indicates that the potential of Eco 3′ to form a stem-loop structure did not provide an advantage with respect to inhibition efficacy, which suggests that the mechanism underlying Eco 3′ inhibition does not mimic that of the CopA–CopT interaction.

In addition to the catalytic RNA subunit, bacterial RNase P enzymes require a small basic protein subunit for in vivo function.[1–3] We therefore tested the effect of the 15-mer on the processing activity of reconstituted RNase P holoenzyme under conditions that make RNA-alone activity negligible (see the Methods section and Figure 7). Upon simultaneous addition of

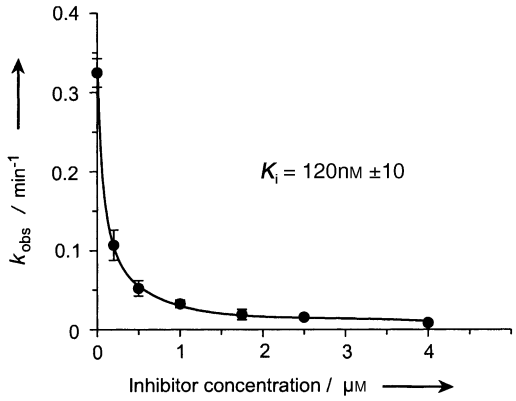

Figure 7. *Inhibiton of RNase P holoenzyme at different concentrations of 15-mer. Mean values are based on three independent experiments; for experimental details, see the Methods section.*

15-mer and ptRNA, that is, under conditions where inhibitor and substrate compete for binding to the P15 loop region, a K_i value of 120 nM was determined. This result demonstrates that inhibition by the 15-mer is not restricted to the RNase P RNA-alone reaction.

Theoretical design of antisense oligonucleotides

Major efforts in antisense research have been devoted to the inhibition of mRNAs by DNA oligonucleotides.[22] As a consequence, comparable experience is missing for stable RNAs, such as RNase P RNA, which fold into very compact secondary and tertiary structures. In recent years, computer-based theoretical approaches for the design of effective antisense oligonucleotides have been developed.[15, 23] We used such an algorithm to design several DNA antisense oligonucleotides (each 18–20 nt in length) directed at regions in *E. coli* RNase P RNA predicted to have the best hybridization efficacy. The initial step applied to the design of oligonucleotides against mRNA targets, namely prediction of RNA secondary structure, was omitted since the secondary structure of *E. coli* RNase P RNA is well established.[7] The tested DNA oligonucleotides are depicted within the secondary structure of *E. coli* RNase P RNA in Figure 8A, along with the RNA 15-mer (see also Figure 5), which was analyzed for comparison. All DNA oligonucleotides were tested at a concentration of 1 μM (100-fold molar excess over *E. coli* RNase P RNA) under the same experimental conditions as described in the legend of Figure 3. Oligonucleotides directed against the P10/11-J11/12 region (P11a, b, c) showed the best inhibition performance among those designed in this second approach (Figure 8B). Based on our finding that Eco 3′ RNA was a far more potent inhibitor than Eco 3′ DNA (Figure 4), we tested RNA versions of oligonucleotides P11a–c. At a concentration of 20 nM (twofold molar excess over *E. coli* RNase P RNA), all three do indeed show improved inhibition efficiency and reduce the processing rate to less than 50% (Figure 9), which suggests that the dissociation constants K_d for binding of these RNA oligonucleotides to *E. coli* RNase P RNA are below 20 nM.

Guerrier-Takada and Altman[24] designed DNA oligonucleotides (17–22 nt in length) targeting nt 56–74, 119–138, 347–363, and 356–377 of *E. coli* RNase P RNA. These oligonucleotides were tested for their affinity to, but not inhibition of RNase P RNA. The oligonucleotide targeting nt 119–138 (P10/11-J11/12) showed the highest affinity, with a K_d value in the low nanomolar range.[24] These results are consistent with our findings. Based on our experience with the CCA binding region,[25] we are also confident that an optimization process (variation of length and positioning of 5′ and 3′ ends), combined with a ribose-phosphate backbone, will reveal more potent variants of oligonucleotides P11a–c for invasion of the P10/11-J11/12 region (Figure 8A). As the P15 loop, the P10/11-J11/12 region directly interacts with ptRNA substrates.[26–33] Thus, both the P15 and P10/11-J11/12 regions seem to be promising target sites because 1) they are sufficiently interspersed with nonhelical sequence elements, 2) they are assumed to be readily accessible at the surface of RNase P RNA, and 3) antisense oligonucleotide binding directly interferes with substrate docking to these two regions.

Methods

RNA and DNA oligonucleotides: HPLC-purified RNA oligonucleotides were either synthesized as previously described[34] or purchased from IBA (Göttingen, Germany). DNA oligonucleotides were purchased from Invitrogen (Karlsruhe, Germany). Further purification of oligonucleotides was performed on denaturing polyacrylamide gels, oligonucleotides were localized by UV shadowing, excised from the gel, eluted overnight at 4 °C in tris(hydroxymethyl)aminomethane (Tris)-HCl (200 mM, pH 7.1) and ethylenediaminetetraacetate (EDTA;

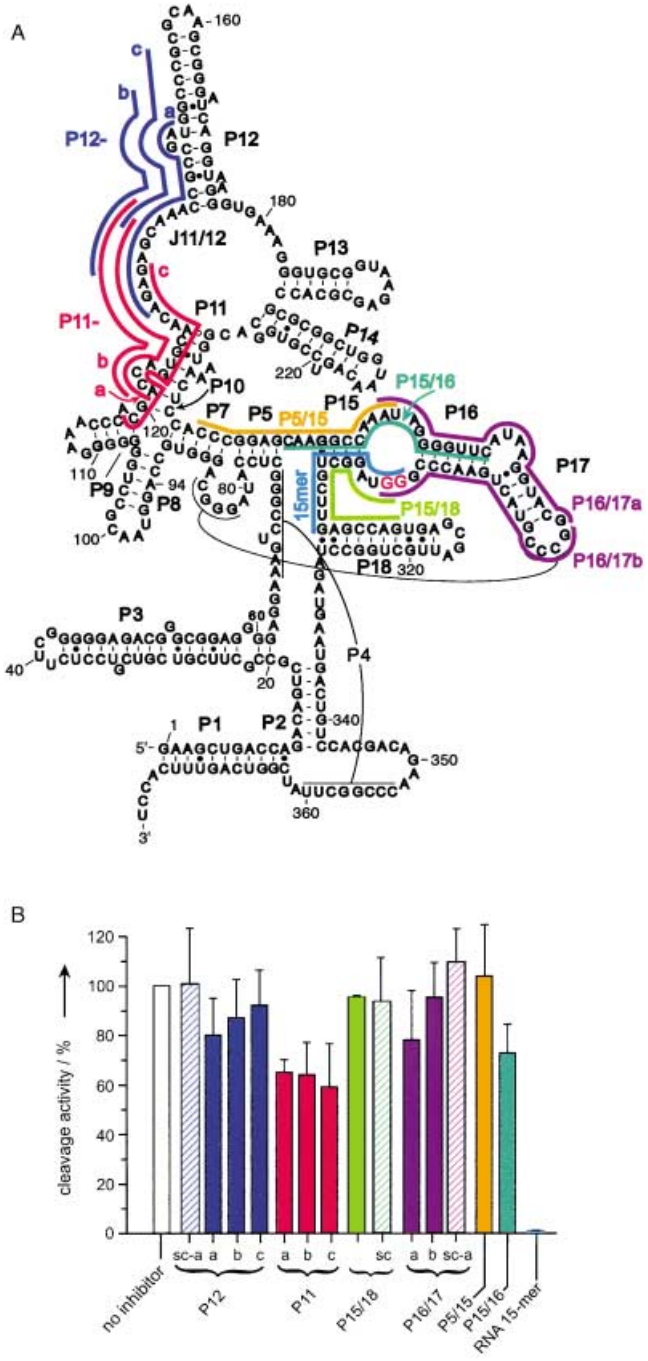

Figure 8. *A) Designed DNA antisense oligonucleotides (each 18 – 20 nt in length) directed against different sites in* E. coli *RNase P RNA and predicted to have the best hybridization efficacy according to target site selection criteria previously reported.[15, 23] B) Effects of DNA oligonucleotides on ptRNA^{Gly} processing by* E. coli *RNase P RNA. For assay conditions, see the legend of Figure 3 and the Methods section. Hatched bars, scrambled (sc) versions of DNA oligonucleotides P12a, P15/18, and P16/17a (see the Methods section; for the RNA 15-mer, see Figure 5). Cleavage activity values are based on three independent experiments. In each individual experimental series, data recorded in the presence of oligonucleotide were related to the corresponding control activity in the absence of inhibitor. Errors indicate fluctuations in activity normalized to the corresponding control (without inhibitor).*

1 mM), and recovered by ethanol precipitation in the presence of NaOAc (75 mM, pH 6.7). The following RNA oligonucleotides were used in this study: Eco 5′: 5′-ACUGUCCUUUACCCGGGUU-

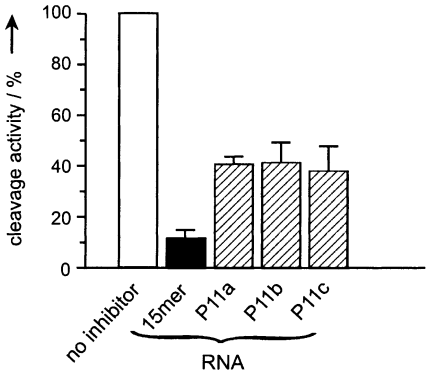

Figure 9. *Inhibition of ptRNA^{Gly} processing by* E. coli *RNase P RNA in the presence of RNA variants of oligonucleotides P11a, P11b, and P11c (see Figure 8). Assays were conducted as described in the legend of Figure 3 and the Methods section, except that the oligonucleotide concentration was 20 nM; the RNA 15-mer is shown for comparison, as in Figure 8.*

CAGU; Eco 3′: 5′-CAAGCAGCCUACCAGCUACCUUG: Mhyo 5′: 5′-CCUAUUUUUUUUACCAAAAUUUAGG; Mhyo 3′: 5′-GGGCUCC-CUUACCGGAUACCC; Eco 3′ AA: 5′-CAAGCAGCCUAAAAGCUAC-CUUG; Eco 3′ UU: 5′-CAAGCAGCCUAUUAGCUACCUUG; 15 -mer: 5′-CAAGCAGCCUACCAG; RNA P11a: 5′-GCUCUCUGUUGCACUG-GU; RNA P11b: 5′-UGCUCUCUGUUGCACUGG; RNA; P11c: 5′-CUCUGUUGCACUGGUCGU. The DNA oligonucleotides used have the following sequences: P15/18: 5′-CTGGCTCAAGCAGCC-TAC; P16/17b: 5′-CCCGGGTTCAGTACGGGC; scrambled (sc) P15/18: 5′-CCCTGGTGGTAACAACCC; P16/17a: 5′-CGTACCTTAT-GAACCCCTAT; P5/15: 5′-ATTTGGCCTTGCTCCGGG; P15/16: 5′-GAACCCCTATTTGGCCTTG; scP16/17a: 5′-AACCCCTTGAAGTTT-CCCAT; P12a: 5′-ATCGGCGGTTTGCTCTCT; P12b: 5′-GCCATCGG-CGGTTTGCTC; P12c: 5′-CGGGCCATCGGCGGTTTG; P11a: 5′-GCT-CTCTGTTGCACTGGT; P11b: 5′-TGCTCTCTGTTGCACTGG; P11c: 5′-CTCTGTTGCACTGGTCGT; scP12a: 5′-GCCCTATGTCTGTGTCTG; Eco 5′ DNA: 5′-ACTGTCCTTTACCCGGGTTCAGT; Eco 3′ DNA: 5′-CAAGCAGCCTACCAGCTACCTTG.

Enzymatic RNA synthesis and 5′-[^{32}P] end labeling: The ptRNA^{Gly} substrate and RNase P RNAs were synthesized by T7 run-off transcription essentially as previously described[10]: ptRNA^{Gly} from plasmid pSBpt3′hh linearized with BamHI,[11] *E. coli* RNase P RNA from plasmid pDW98 linearized with BsaAI,[11] *M. hyopneumoniae* RNase P RNA from plasmid pHyoP linearized with XbaI,[17] *T. thermophilus* RNase P RNA from plasmid pT7M1HB8 linearized with EheI,[35] and *B. subtilis* RNase P RNA from plasmid pDW66 linearized with DraI.[36] 5′ end labeling was performed as previously described.[11] RNAs were purified by denaturing polyacrylamide gel electrophoresis (see above).

Kinetics: Processing assays catalyzed by RNase P RNA were performed under multiple turnover conditions (10 nM RNase P RNA, 100 nM ptRNA^{Gly} substrate including trace amounts of 5′-[^{32}P] end-labeled ptRNA^{Gly}) in buffer I (0.1 M NH_4OAc, 0.1 M $Mg(OAc)_2$, 50 mM 2-[4-(2-hydroxyethyl)-1-piperazinyl]ethanesulfonic acid (HEPES), pH 7.0). RNase P RNAs were preincubated in the presence or absence of the inhibitor oligonucleotides in cleavage assay buffer I for 40 min (if not stated otherwise) at 37 °C (RNase P RNA from *T. thermophilus* was additionally preincubated for 10 min at 55 °C in buffer I before this preincubation step). Processing reactions were started by addition of substrate that had been preincubated

separately for 5 min at 55 °C and 20 min at 37 °C in buffer I. Aliquots were withdrawn at various time points and analyzed by electrophoresis in 20% polyacrylamide/8 M urea gels. Data analysis and calculation of turnover rates of cleavage (k_{obs}) were performed essentially as previously described.[11]

RNase P holoenzyme kinetics studies were performed under multiple turnover conditions in 0.9 × buffer II (1 × buffer 110 mM KCl, 8 mM $MgCl_2$, 40 mM HEPES, pH 6.9). For the reconstitution of holoenzyme, *E. coli* RNase P RNA (0.2 μM) was incubated with the *B. subtilis* RNase P protein subunit (0.2 μM) in 1 × buffer II for 10 min at 37 °C. Glycerol (10% of the incubation volume) was then added and the mixture was kept on ice for 10 min. Aliquots (1.4 μL) were withdrawn, frozen in liquid nitrogen and stored at −80 °C. For kinetics, 1 × buffer II was prewarmed to 37 °C and added to the frozen holoenzyme aliquot. After 2 min preincubation at 37 °C, the RNA 15-mer (in 2 μL H_2O) was added and the reaction was started immediately (within 10 seconds) by addition of ptRNA (in 1 × buffer II) preincubated separately (see above; total reaction volume 26 μL). Samples were withdrawn at various time points and analyzed as described above.

Bioinformatics—design of antisense oligonucleotides: To design DNA antisense oligonucleotides against *E. coli* RNase P RNA, we first selected target RNA regions in RNase P RNA whose structural characteristics potentially favor oligonucleotide binding. For this purpose, we used rules that we deduced from a systematic computational approach to designing antisense oligonucleotides that effectively target mRNAs in living cells.[15, 23] Current secondary and tertiary structure models of *E. coli* RNase P RNA served as the basis for oligonucleotide design.[7, 37] In a second step, the sequences of antisense oligonucleotides (18–20 nucleotides in length) were chosen such that their 5′ or 3′ ends were directed close to the central portion of the target RNA structure motifs assumed to be accessible (Figure 8A). Scrambled oligonucleotides were used as controls. Subsequently, sequence-specific characteristics of the designed oligonucleotides were examined. Exclusion criteria were: 1) significant matches of oligonucleotide sequence to unrelated bacterial or human coding regions (Nucleotide Blast software[38]), 2) a high potential for dimer formation and intramolecular folding (Oligo version 3.4 program[39]), and 3) unfavorable sequence motifs.[15]

Acknowledgements

We are grateful to Markus Paaschburg for kinetic measurements, Leif A. Kirsebom for providing plasmid pHyoP, and Georg Sczakiel for fruitful discussion. This work was supported by the Deutsche Forschungsgemeinschaft (Grant no. HA 1672/7-3).

Keywords: antisense agents · DNA · oligonucleotides · RNA · RNase P

[1] D. N. Frank, N. Pace, *Annu. Rev. Biochem.* **1998**, *67*, 153–180.
[2] S. Altman, L. A. Kirsebom in *The RNA World* (Eds.: R. F. Gesteland, T. Cech, J. F. Atkins), Cold Spring Harbor Laboratory Press, Cold Spring Harbor, NY, 2nd ed. **1999**, pp. 351–380.
[3] A. Schön, *FEMS Microbiol. Rev.* **1999**, *23*, 391–406.
[4] N. Jarrous, *RNA* **2002**, *8*, 1–7.
[5] S. Xiao, F. Scott, C. A. Fierke, D. R. Engelke, *Annu. Rev. Biochem.* **2002**, *71*, 165–189.
[6] K. Kobayashi et al., *Proc. Natl. Acad. Sci. USA* **2003**, *100*, 4678–4683.
[7] J. W. Brown, *Nucleic Acids Res.* **1998**, *26*, 351–352.
[8] H. L. True, D. W. Celander, *J. Biol. Chem.* **1998**, *273*, 7193–7196.
[9] L. A. Kirsebom, S. G. Svärd, *EMBO J.* **1994**, *13*, 4870–4876.
[10] C. Heide, T. Pfeiffer, J. M. Nolan, R. K. Hartmann, *RNA* **1999**, *5*, 102–116.
[11] S. Busch, L. A. Kirsebom, H. Notbohm, R. K. Hartmann, *J. Mol. Biol.* **2000**, *299*, 941–951.
[12] H. Dong, L. A. Kirsebom, L. Nilsson, *J. Mol. Biol.* **1996**, *261*, 303–308.
[13] T. D. Eubank, R. Biswas, M. Jovanovic, A. Litovchick, A. Lapidot, V. Gopalan, *FEBS Lett.* **2002**, *511*, 107–112.
[14] H.-Y. Tsai, B. Masquida, R. Biswas, E. Westhof, V. Gopalan, *J. Mol. Biol.* **2003**, *325*, 661–675.
[15] R. Kretschmer-Kazemi Far, W. Nedbal, G. Sczakiel, *Bioinformatics* **2001**, *17*, 1058–1061.
[16] E. S. Haas, A. B. Banta, J. K. Harris, N. R. Pace, J. W. Brown, *Nucleic Acids Res.* **1996**, *24*, 4775–4782.
[17] S. G. Svärd, J. G. Mattsson, K. E. Johansson, L. A. Kirsebom, *Mol. Microbiol.* **1994**, *11*, 849–859.
[18] S. G. Svärd, U. Kagardt, L. A. Kirsebom, *RNA* **1996**, *2*, 463–472.
[19] F. A. Kolb, C. Malmgren, E. Westhof, C. Ehresmann, B. Ehresmann, E. G. Wagner, P. Romby, *RNA* **2000**, *6*, 311–324.
[20] F. A. Kolb, H. M. Engdahl, J. G. Slagter-Jager, B. Ehresmann, C. Ehresmann, E. Westhof, E. G. Wagner, P. Romby, *EMBO J.* **2000**, *19*, 5905–5915.
[21] W. F. Lima, B. P. Monia, D. J. Ecker, S. M. Freier, *Biochemistry* **1992**, *31*, 12055–12061.
[22] G. Sczakiel, *Front Biosci.* **2000**, *5*, d194–201.
[23] V. Patzel, U. Steidl, R. Kronenwett, R. Haas, G. Sczakiel, *Nucleic Acids Res.* **1999**, *27*, 4328–4334.
[24] C. Guerrier-Takada, S. Altman, *Biochemistry* **1993**, *32*, 7152–7161.
[25] H. Gruegelsiepe, D. K. Willkomm, O. Goudinakis, K. Hartmann, *ChemBioChem* **2003**, *4*, 1049–1056.
[26] W. H. McClain, C. Guerrier-Takada, S. Altman, *Science* **1987**, *238*, 527–530.
[27] D. Kahle, U. Wehmeyer, G. Krupp, *EMBO J.* **1990**, *9*, 1929–1937.
[28] D. L. Thurlow, D. Shilowski, T. L. Marsh, *Nucleic Acids Res.* **1991**, *19*, 885–891.
[29] A. Loria, T. Pan, *Biochemistry* **1997**, *36*, 6317–6325.
[30] J. M. Nolan, D. M. Burke, N. R. Pace, *Science* **1993**, *261*, 762–765.
[31] M. E. Harris, J. M. Nolan, A. Malhotra, J. W. Brown, S. C. Harvey, N. R. Pace, *EMBO J.* **1994**, *13*, 3953–3963.
[32] T. Pan, A. Loria, K. Zhong, *Proc. Natl. Acad. Sci. USA* **1995**, *92*, 12510–12514.
[33] C. Heide, R. Feltens, R. K. Hartmann, *RNA* **2001**, *7*, 958–968.
[34] A. Nolte, S. Klussman, S. Lorenz, R. Bald, C. Betzel, Z. Dauter, K. Wilson, J. P. Furste, V. A. Erdmann, *FEBS Lett.* **1995**, *374*, 292–294.
[35] R. Feltens, M. Gössringer, D. K. Willkomm, H. Urlaub, R. K. Hartmann, *Proc. Natl. Acad. Sci. USA* **2003**, *100*, 5724–5729.
[36] J. M. Warnecke, R. Held, S. Busch, R. K. Hartmann, *J. Mol. Biol.* **1999**, *290*, 433–445.
[37] C. Massire, L. Jaeger, E. Westhof, *J. Mol. Biol.* **1998**, *279*, 773–793.
[38] http://www.ncbi.nlm.nih.gov
[39] W. Rychlik, R. E. Rhoads, *Nucleic Acids Res.* **1989**, *21*, 8543–8551.
[40] A. Loria, T. Pan, *RNA* **1996**, *2*, 551–563.
[41] W. D. Hardt, J. Schlegl, V. A. Erdmann, R. K. Hartmann, *Nucleic Acids Res.* **1993**, *21*, 3521–3527.
[42] L. A. Kirsebom in *The Many Faces of RNA* (Eds.: D. S. Eggleston, C. D. Prescott, N. D. Pearson), Academic Press, UK, **1998**, pp. 127–144.

Received: May 21, 2003 [F674]

